NEVER REVISIT: CONTINUOUS EXPLORATION IN MULTI-AGENT REINFORCEMENT LEARNING

Anonymous authors
Paper under double-blind review

ABSTRACT

Recently, intrinsic motivations are wildly used for exploration in multi-agent reinforcement learning. We discover that coming with intrinsic rewards is the issue of revisitation – the relative values of intrinsic rewards, estimated based on neural networks, fluctuate during learning, causing failures of rediscovering promising areas after detachment of exploration. Consequently, agents risk exploring some sub-spaces repeatedly and being stacked nearing the fixed initial point. In this paper, we formally define the concept of revisitation, based on which we propose an observation-distribution matching approach to detect the appearance of revisitation. To avoid it, we add branches to agents' local Q-networks and the mixing network to separate sub-spaces that have already been revisited for sufficient policy representation capacity. Furthermore, we use historical samples of joint observation to adjust intrinsic rewards to reduce the probability of and penalize the occurrence of revisitation. By virtue of these advances, our method achieves superior performance on three challenging Google Research Football (GRF) scenarios and three StarCraft II micromanagement (SMAC) maps with sparse rewards.

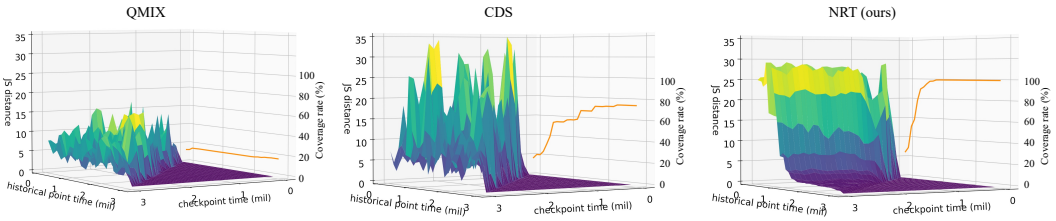

Figure 1: The issue of revisitation. During learning, we will store the joint observation distribution induced by the joint policy π every 100k time steps, named historical point time. Meanwhile, for every 100k time step, we will calculate the JS distance between the current distribution and all historical points, named checkpoint time. Experiments are carried out on a 6×12 maze task introduced in Sec. 4. **Left**: Basic exploration scheme (QMIX (Rashid et al., 2018) with ϵ-greedy exploration) achieves a coverage rate of the joint observation space less than 20%. **Middle**: Adding CDS (Li et al., 2021) intrinsic incentives improves the coverage rate to 80%. However, the fluctuating JS distances indicate that agents are periodically revisiting some sub-spaces. Consequently, most samples are wasted on revisitation. **Right**: Revisitation is avoided based on our method, and the JS distances are large and stable before converging to an optimal strategy, indicating continuous exploration achieved by our approach.

1 INTRODUCTION

Multi-agent cooperation is ubiquitous in real-world problems, such as sensor networks (Zhang & Lesser, 2013) and traffic light control (Zhang et al., 2019). To introduce intelligence into multi-agent systems and achieve sophisticated cooperative behavior, multi-agent reinforcement learning (MARL) has been gaining increasing interest in recent years. Advanced MARL methods have largely pushed forward the performance of machine learning algorithms on tasks such as StarCraft II micromanagement (Rashid et al., 2018; Wang et al., 2021b), Hanabi (Bard et al., 2020; Foerster et al., 2019), and robotic control (Kurin et al., 2020).

Despite these achievements, a problem persists and prevents MARL from extending successfully to more complex problems. The action-observation space grows exponentially with the number of agents, and the efficiency of exploration strategies in such search spaces largely limits the learning efficiency of MARL algorithms. Basic exploration (Wang et al., 2020b) schemes, like ϵ-greedy, adopted by many previous works (Wang et al., 2021a; Yu et al., 2021; de Witt et al., 2020) appear to struggle even in tasks with a moderate number of agents. For example, in a 6×12 maze game with two agents (Fig. 4 (b)), QMIX (Rashid et al., 2018) using independent search can only cover less than 20% of the joint observation space (Fig. 1 left) and struggles to find any rewards.

Various intrinsic motivations are introduced into MARL algorithms to enhance their exploration ability by encouraging interaction among agents (Wang et al., 2020b), maximizing a measurements of behavioral randomness (Houthooft et al., 2016; Mahajan et al., 2019; Gupta et al., 2021), and spurring individuality (Jiang & Lu, 2021) and diversity (Li et al., 2021). These methods significantly enlarge the sub-space that can be explored. For example, the coverage rate increases from $\sim 20\%$ to $\sim 80\%$ using the CDS (Li et al., 2021) diversity-encouragement incentives (Fig. 1 middle). However, in this paper, we find that coming with the augmented exploration is a ***revisitation*** problem that severely hurts the expected exploration ability and prevents learning efficiently.

Revisitation refers to the situation where, with an enlarged exploration space, agents forget the areas they have visited before after the detachment of exploration, causing them to return and re-explore. In this way, agents are stacked nearing the fixed initial point and can not explore continuously. Meanwhile, revisitation in some sub-spaces can repeatedly happen, making this issue more detrimental. For example, in Fig. 1 (middle), we present the empirical joint observation distribution induced by CDS (Li et al., 2021) policies at different training time steps. It can be observed that similar distributions occur periodically during learning, and the algorithm wastes most training samples on unvalued, revisited experiences.

In this paper, we give a formal definition for revisitation in multi-agent settings, based on which we propose a framework for solving this issue. Intuitively, we consider revisitation occurs because of (1) insufficient policy representation capacity causing forgetting and (2) ineffective intrinsic motivations after the detachment (Ecoffet et al., 2019) of exploration. To handle the first problem, we add branches to agents' local Q-networks and the mixing network when revisitation occurs to achieve a dynamically growing neural network structure. To handle the second problem, we use historical samples of joint observations to adjust intrinsic rewards. Taking benefit of our correction mechanism, we can prevent revisitation from occurring to avoid an excessive number of branches in the network. Meanwhile, for each revisitation, we further introduce a KL divergence to penalize it to happen again.

Based on the above merits for detecting and preventing revisitation, our approach NRT (**N**ever **R**evisi**t**) achieves nearly 100% coverage rate on the maze task (Fig. 1 right). Furthermore, we benchmark our approach on both Google Research Football (GRF, Kurach et al. (2020)) and SMAC (Samvelyan et al., 2019) in the sparse reward setting, and find that NRT significantly pushes forward state of the art. Ablation studies show that adding branches is the most important component in revisitation avoidance and performance improvement for challenging tasks. At the same time, the proposed intrinsic reward adjustment modules are critical in achieving continuous exploration.

2 Background

In this paper, we formulate multi-agent coordination tasks as Dec-POMDP Oliehoek et al. (2016), which can be defined as a tuple $\mathcal{G} = \langle I, S, A, P, R, O, n, \gamma \rangle$, where I is the set of agents, S is the state space, A is the action space, P is the transition function, R is the reward function, O is the observation space, n is the number of agents, and $\gamma \in [0, 1)$ is the discount factor. During sampling, each agent $i \in I$ observes its unique information o_i and selects an action $a_i \in A$ independently. According to the joint action $\boldsymbol{a}$ and environment transition function $P(s'|s, \boldsymbol{a})$, the environment transfers to a new state s' and provides a reward that is shared across all agents.

2.1 Centralized Training with Decentralized Execution

Our approach follows a recently advanced multi-agent optimization framework of centralized training with decentralized execution (CTDE) Lowe et al. (2017); Foerster et al. (2018); Sunehag et al. (2018); Rashid et al. (2018). In this framework, each agent executes only based on its local action-observation

history. This distributed decision-making tackles the exponentially growing joint action space. For stable optimization, agents are trained in a centralized manner with access to global information to achieve reasonable credit assignment across agents. The individual-global-max (IGM) principle Son et al. (2019) further guarantees the consistency between the local and global Q-function based on value factorization. With the above advantages, some algorithms Son et al. (2020); Wang et al. (2021a); Ma et al. (2021) have achieved remarkable progress in challenging cooperation tasks.

2.2 CDS

Although the CTDE framework has been proven to accelerate training with value factorization, it still has to face a giant search space. Diversity in exploration is required for sophisticated cooperation. Li et al. (2021) introduced CDS, which achieves diversity when necessary via shared experiences. Some of the most salient novelties are: (1) Introduce an intrinsic reward function as shown in Eq. 1 based on $I^{\pi}(\tau_T; id)$ to encourage specialty of individual trajectories. (2) Provide an independent Q-network for each agent to estimate local Q-value after combining with one shared Q-network. (3) Add an L1 regularization on independent Q-values to encourage sharing crucial knowledge while keeping enough policy representation capacity of necessary diversity.

$$\begin{aligned} r_{\text{CDS}}^{I} = \beta E_{id}\left[\beta_2 D_{\text{KL}}\left(\text{SoftMax}\left(\beta_1 Q\left(\cdot \mid \tau_t, id\right)\right) | p\left(\cdot \mid \tau_t\right)\right)\right. \\ \left. +\beta_1 \log q_{\phi}\left(o_{t+1} \mid \tau_t, a_t, id\right) - \log p\left(o_{t+1} \mid \tau_t, a_t\right)\right], \end{aligned} \tag{1}$$

where id is the identity of each agent, β, β_1 and β_2 are hyper-parameters introduced in CDS, and $\tau_T = (o_0, a_0, o_1, \ldots, o_T)$ is the variable of one agent's trajectory. In this paper, we use r_{CDS}^{I} as an example to expose and solve one crucial potential problem of existing intrinsic motivation methods, revisitation as shown in Fig. 1 (middle).

3 METHOD

3.1 REVISITATION DETECTION

We first define the concept of ***revisitation*** in multi-agent settings. Our definition is based on the empirical joint observation distribution induced by the joint policy $\boldsymbol{\pi}$: $\rho_{\boldsymbol{\pi}}(\boldsymbol{o}) = \mathbb{E}_{\boldsymbol{\pi}}[\frac{1}{T}\sum_{t=0}^{T} \mathbf{1}_{\boldsymbol{o}_t=\boldsymbol{o}}]$. Intuitively, when $\rho_{\boldsymbol{\pi}}(\boldsymbol{o})$ changes significantly, the agent team starts to explore a new sub-space. Still, if, after a significant change, $\rho_{\boldsymbol{\pi}}(\boldsymbol{o})$ degenerates to a distribution that has occurred before, revisitation happens. Formally, we have the following definition:

Definition 1. *A δ-revisitation occurs at time step t if there exists a time step $t'' < t$ so that*

1. $\max_{t' \in (t'', t)} D_{\text{JS}}\left[\rho_{\boldsymbol{\pi}_{t''}}(\boldsymbol{o}) \| \rho_{\boldsymbol{\pi}_{t'}}(\boldsymbol{o})\right] > \delta$;
2. $D_{\text{JS}}\left[\rho_{\boldsymbol{\pi}_{t''}}(\boldsymbol{o}) \| \rho_{\boldsymbol{\pi}_{t}}(\boldsymbol{o})\right] < \delta$.

Here, D_{JS} is the Jensen-Shannon distance between two distributions. The first condition describes the ability of many multi-agent exploration algorithms. As the learning progresses, agents are encouraged to explore new sub-spaces, leading to a shift in the empirical joint observation distribution. The second condition depicts the occurrence of revisitation. After exploring a new sub-space for a while, the agents may forget previously learned knowledge, possibly due to limited network representative capacity, and start to re-explore previously visited sub-spaces.

Under discrete observation space, we can estimate $\rho_{\boldsymbol{\pi}}(\boldsymbol{o})$ with the Monte Carlo (MC) method. However, in continuous observation space, it is intractable to use MC. In practice, we estimate the joint observation distribution $\rho_{\boldsymbol{\pi}}(\boldsymbol{o})$ using an a variational auto-encoder parameterized by ξ, by minimizing the evidence lower bound:

$$\mathcal{L}_{\rho}(\xi) = \mathbb{E}_{\text{q}(z|\boldsymbol{o};\xi)}[\log p(\boldsymbol{o}, z; \xi) - \log q(z \mid \boldsymbol{o}; \xi)], \tag{2}$$

where z is a latent variable to reconstruct $\boldsymbol{o}$, and $p_{\xi}(\boldsymbol{o}) = \int p_{\xi}(\boldsymbol{o} \mid z)p(z)\mathrm{d}z \approx \frac{1}{L}\sum_{i=1}^{L} p_{\xi}(\boldsymbol{o} \mid z_i)$ for $z_i \sim p(z)$, where $p(z)$ is a prior of the latent variable vector, which is modeled by a standard Gaussian distribution $\mathcal{N}(z \mid \mathbf{0}, \mathbf{I})$ and L is fixed as 32 in this paper.

During training, for every 100k time step, we store the current joint observation distribution estimator p_{ξ_t} into a buffer, and check for each previous version $p_{\xi_{t''}}$ whether they satisfy the two conditions listed in Definition 1. If the conditions are satisfied, we call (t'', t', t) a ***revisitation tuple*** and store $(\rho_{\boldsymbol{\pi}_{t''}}(\boldsymbol{o}), \rho_{\boldsymbol{\pi}_{t'}}(\boldsymbol{o}), \rho_{\boldsymbol{\pi}_t}(\boldsymbol{o}))$ with $(\rho_{\boldsymbol{\pi}_{t''}}(o_i), \rho_{\boldsymbol{\pi}_{t'}}(o_i), \rho_{\boldsymbol{\pi}_t}(o_i))$ for each agent $i \in I$, where $\rho_{\boldsymbol{\pi}}(o_i) = \mathbb{E}_{\boldsymbol{\pi}}\left[\frac{1}{T}\sum_{t=0}^{T} \mathbf{1}_{o_{i,t}=o_i}\right]$ is estimated along with $\rho_{\boldsymbol{\pi}}(\boldsymbol{o})$.

3.2 Augmentation of the Training Framework

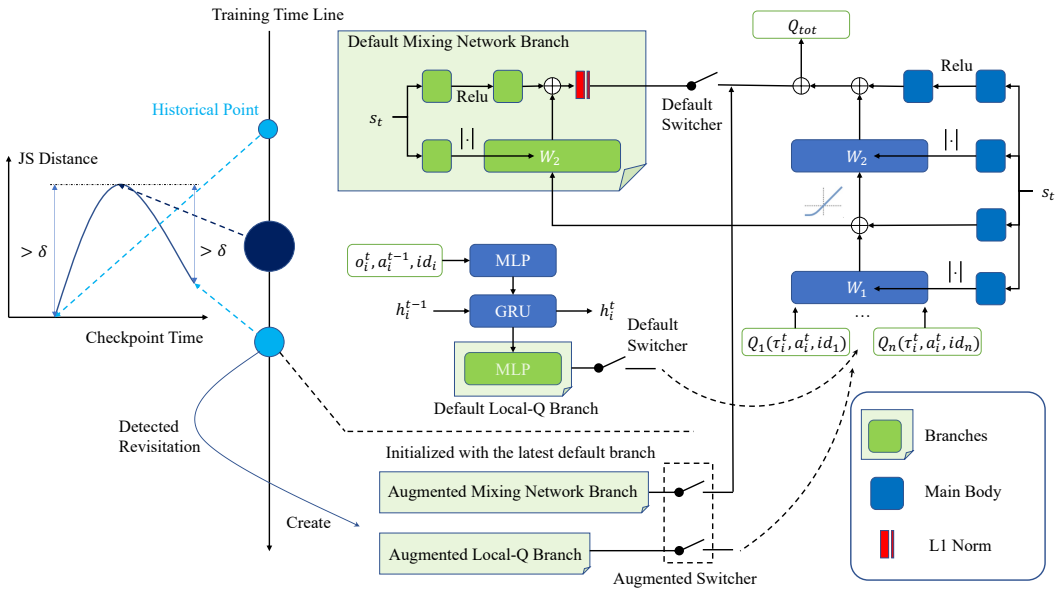

Figure 2: Dynamic augmentation of NRT (**N**ever **R**evisi**t**)'s neural network structure (using one detected revisitation as an example).

To achieve sufficient policy representation capacity for handling revisitation while benefiting from parameter sharing, we dynamically augment partial neural networks (branches) as shown in Fig. 2. In this paper, we follow the CTDE framework as discussed in Sec. 2.1 with a mixing network as QMIX (Rashid et al., 2018), whose weights are produced by separate hyper networks with an input of state and are followed by an absolute activation function to ensure the IGM principle. Starting from the beginning of training, we provide a default mixing network branch (a part of the mixing network), a default local-Q branch (the last layer of local Q-networks), and the main body of our neural networks. The main body is painted blue, while branches are painted green. After one detection of revisitation, we will create a related augmented mixing network branch and a related augmented local-Q branch with the same structure as the default ones to increase representational capacity. Their parameters are initialized according to the latest default branches.

Along with our dynamic augmentation structure is a question about how to switch different branches. Formally, for b th augmented branch, we define the associated joint observation set Ω_b based on the definition of related revisitation tuple (t''_b, t'_b, t_b) introduced in Sec. 3.1.

$$\Omega_b = \{\boldsymbol{o} || \log \rho_{\boldsymbol{\pi}_{t''_b}}(\boldsymbol{o}) - \log \rho_{\boldsymbol{\pi}_{t'_b}}(\boldsymbol{o})\}| > \delta\} \cap \{\boldsymbol{o} || \log \rho_{\boldsymbol{\pi}_{t''_b}}(\boldsymbol{o}) - \log \rho_{\boldsymbol{\pi}_{t_b}}(\boldsymbol{o})\}| < \delta\}. \quad (3)$$

However, during decentralized execution, one agent can only obtain its observation. Thus, we further introduce the marginal set Ω_b^i for each agent $i \in I$ as shown in Eq. 4. If agent i's local observation $o_i \in \Omega_b^i$, the related b th augmented local-Q branch will be activated for both sampling and training. If none of augmented branches is activated or created, agents will choose the default branch.

$$\Omega_b^i = \{o_i || \log \rho_{\boldsymbol{\pi}_{t''_b}}(o_i) - \log \rho_{\boldsymbol{\pi}_{t'_b}}(o_i)\}| > \frac{\delta}{n}\} \cap \{o_i || \log \rho_{\boldsymbol{\pi}_{t''_b}}(o_i) - \log \rho_{\boldsymbol{\pi}_{t_b}}(o_i)\}| < \frac{\delta}{n}\}. \quad (4)$$

There are two questions coming with Eq. 4, (1) how to switch augmented local-Q branches when o_i belongs to several sets simultaneously, and (2) how to switch augmented mixing network branches when agents switch various local-Q branches. As for question (1), we will check according to the created order and activate the earliest branch. As for question (2), each augmented mixing network branch will be activated only when more than half of agents choose the corresponding augmented local-Q branch. Our neural networks will switch to the default branch if none of augmented branches is activated or created. Because the whole trajectory is spliced from different branches, we expect credit assignments across agents (achieved by the mixing network) to not differ too much for stability. Thus we add an L1 regularization to mixing network branches to encourage them to work only when necessary. More details and the pseudo-code of NRT's sampling process are discussed in Sec. B.1

3.3 Auxiliary Supporting Incentives

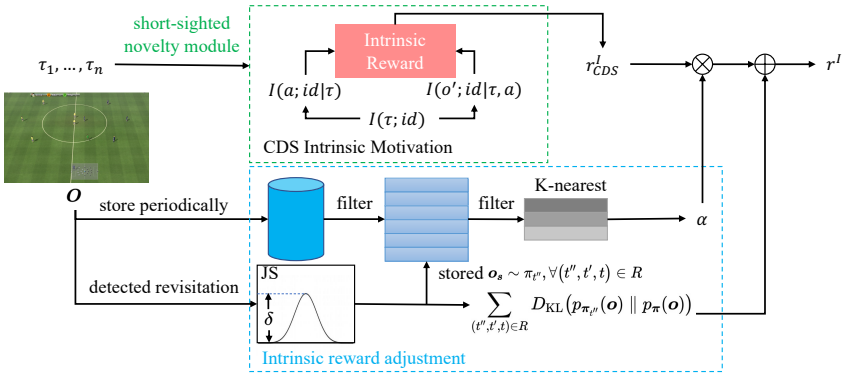

Figure 3: NRT (**N**ever **R**evisi**t**)'s intrinsic reward adjustment modules.

A possible shortcoming of the methods introduced above is that when revisitation occurs frequently, there may be too many branches. To prevent the number of branches from increasing quickly and adjust intrinsic rewards for handling the detachment of exploration, we design adjustment modules for intrinsic motivations to (1) prevent the appearance of revisitation in advance, and (2) penalize the occurrence of revisitation.

To prevent revisitation caused by the detachment of intrinsic motivations, we adjust intrinsic rewards with historical samples of joint observations. In this paper, we periodically store joint observation sequences (every ten episodes) in an independent buffer without deletion. During training, for time efficiency, we form a compact sub-sampling buffer with 10 trajectories from the whole learning period and 5 trajectories from each revisitation's historical point. As inspired by Badia et al. (2020), based on the K-nearest approach, we calculate the weight of intrinsic rewards: $\alpha = \frac{1}{\sqrt{\sum_{o_{\mathcal{N}} \in \mathcal{N}_k(o)} K(o, o_{\mathcal{N}}) + \epsilon}}$, where $\mathcal{N}_k(\boldsymbol{o})$ is the k nearest neighbors of $\boldsymbol{o}$ in the compact buffer, and ϵ is a small constant (0.001) for numeric stability. The kernel function $K(\cdot, \cdot)$ is defined as $K(x, y) = \frac{\epsilon}{d^2(x,y)+\epsilon}$, where d is the Euclidean distance.

For penalizing revisitation, we further introduce $r^p = \sum_{(t'',t',t)\in R} D_{\mathrm{KL}}\left(p_{\boldsymbol{\pi}_{t''}}(\boldsymbol{o}) \| p_{\boldsymbol{\pi}}(\boldsymbol{o})\right)$, where $p_{\boldsymbol{\pi}}$ is the current joint policy. Overall, the intrinsic reward used in our paper is

$$r^I = r^I_{\text{CDS}} \cdot \texttt{clip}(1 + \bar{\alpha}, L_1, L_2) + \beta_p r^p, \tag{5}$$

where $\bar{\alpha} = \frac{\alpha - \mu_e}{\sigma_e}$ is the running average of α, `clip` means we clip the running average so that it is in the range $[L_1, L_2]$, r^I_{CDS} is the intrinsic reward introduced by CDS (Li et al., 2021) as shown in Eq. 1, and β_p is a hyper-parameter tuning the weight of r^p, which is fixed as 0.001 in our experiments.

4 Didactic Example

In this section, we present a maze task (shown in Fig. 5 (b)) to demonstrate the existence of revisitation, its influence on exploration, and how our approach improves learning performance by

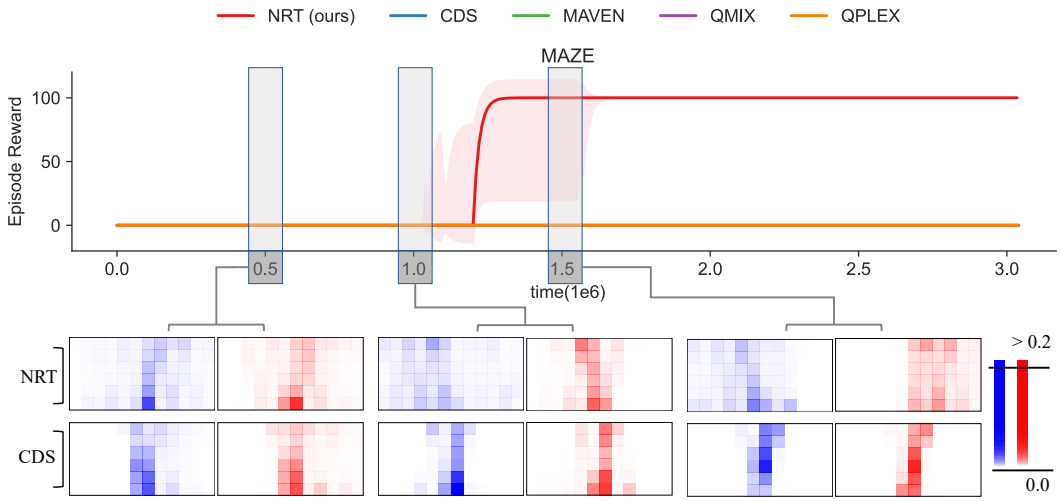

Figure 4: Comparison against baselines with visitation heat maps.

avoiding revisitation. In this task, two agents are initialized at the blue point and are expected to simultaneously reach two red points located in different corners of a 6×12 maze within 50 steps. Each agent can observe its own and teammate's coordinates. The action set of both agents includes one-step movement in four directions and an idle action for doing nothing. Only when agents reach two red points simultaneously, the episode will terminate immediately with a team reward of 100. For any other cases, reward is set to 0.

Fig. 4 shows the comparison of our approach against baseline algorithms, including state-of-the-art value function factorization learning methods (QMIX (Rashid et al., 2018) and QPLEX (Wang et al., 2021a)) and multi-agent exploration algorithms (CDS (Li et al., 2021) and MAVEN (Mahajan et al., 2019)). Experimental results demonstrate the advantage of our approach in exploration, as NRT is the only algorithm that obtains the episode reward of 100.We further provide visitation heat maps of NRT and CDS within three periods ($0 \sim 0.5$M, 0.5M ~ 1.0M, and 1.0M ~ 1.5M). NRT continuously encourage agents to explore further, while agents trained by CDS are stacked nearing the fixed initial points and waste most training samples on revisited experiences after the detachment of previous exploration.

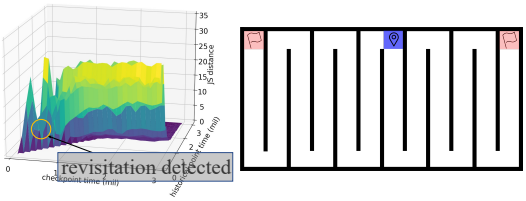

(a)Another perspective of JS distance changing

(b) Environment

Figure 5: Structure of the maze and continuous exploration achieved by our approach.

In Fig. 5 (a), we further show another perspective of the 3D plot of JS distance plot to demonstrate continuous exploration achieved by our approach after detecting revisitation. The circle in Fig. 5 (a) highlights a time step when a revisitation is detected. At this time, our approach (1) adds a new branch as described in Sec. 3.2; (2) ensures that the joint observations where the revisitation happens are sampled when calculating the intrinsic reward; and (3) adds punishment for revisitation. In this way, our approach effectively prevents the reappearance of revisitation, leading to continuous exploration.

5 Experiment

In Sec. 4, we introduce a toy maze environment to illustrate our approach's efficiency of exploration while showing the significant harm of repeat revisitation learned by current advanced multi-agent algorithms. In this section, we will compare our approach against baselines on Google Research Football (GRF) Kurach et al. (2020) and SMAC (Samvelyan et al., 2019) in the sparse reward setting, which are currently the most challenging benchmarks for testing cooperation between agents. We show the median and variance of every evaluation's average performance of our approach, baselines, and ablations tested with three random seeds (seed=0,1,2).

5.1 GRF

The GRF benchmark provides numerous scenarios varying in agent numbers and difficulty. In each scenario, algorithms typically control agents on the left side and play against the built-in AI. In this paper, we use three representative scenarios to demonstrate the significance of considering revisitation. Agents' initial locations for each scenario are shown in Appendix. Following the convention of Kurach et al. (2020) and Li et al. (2021), the state and each agent's observation are based on the official simple 115 representation vector, while observations are established according to relative positions. Each agent has a discrete action space of 19 dimensions, including moving and several basic actions, such as passing and shooting. Environmental rewards are only provided at the end of one episode. Agents will get $+100$ if they score, else get -1.

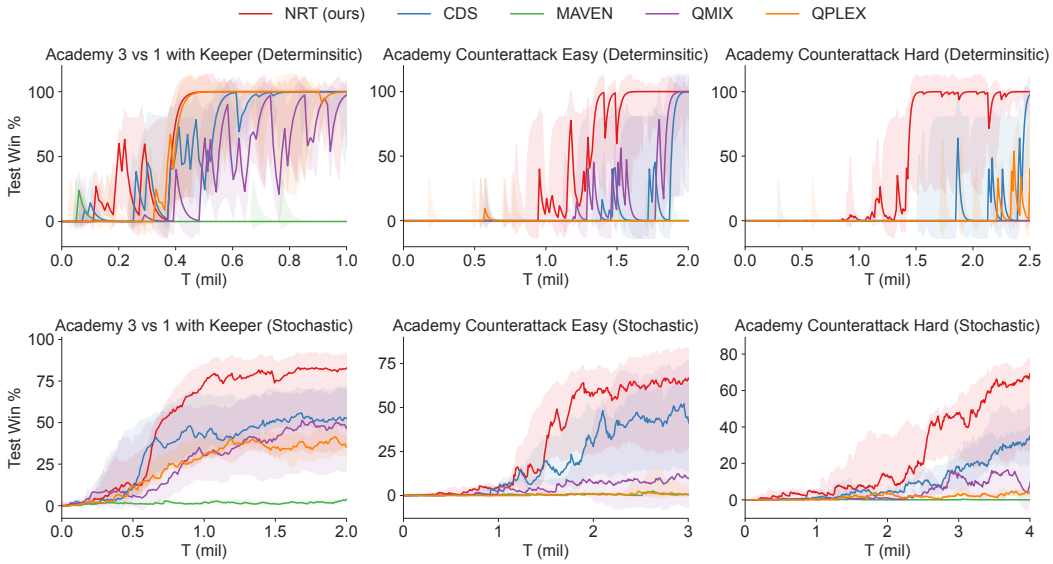

Figure 6: Comparison of our approach against baseline algorithms on GRF with deterministic environment seeds or stochastic environment seeds. We smooth all curves based on the running average. In the deterministic setting, the weight is 0.6, while it is 0.9 in the stochastic counterpart.

Fig. 6 demonstrates the comparison between our approach with baseline algorithms in the deterministic and stochastic settings. Here we first analyze experiment results in the deterministic setting. In `Academy_3_vs_1_with_Keeper`, QPLEX can achieve similar learning efficiency with our approach, while CDS and QMIX can also achieve a 100% winning rate. However, in more complex scenarios, `Academy_Counterattack_Hard` in particular, the outperformance of our approach is obvious, showing the advantages of considering revisitation. In `Academy_3_vs_1_with_Keeper` and `Academy_Counterattack_Easy`, CDS performs similar with QMIX. With our additional supporting incentives based on Q-function restoration, NRT achieves more efficient exploration.

Like the deterministic counterpart, our approach maintains its outperformance in the stochastic setting, as shown in Fig. 6. Because opposing players' behavior might differ across various random environment seeds, the average winning rates during evaluation are nearly impossible to be 100%. In this case, our approach still shows clear superiority in all three scenarios. In challenging scenarios, such as `Academy_Counterattack_Easy`, CDS outperforms QMIX. Following the guidance of our life-long novelty guarantee module, the performance is further raised in all three scenarios. Experiment results illustrate that our approach can tune intrinsic motivations to lead them to more sophisticated policies in complex tasks.

Ablation Study To understand contribution of each component in the proposed NRT framework, we conduct three ablations: (1) ablate augmented branches, (2) ablate auxiliary dynamic weight of intrinsic motivations, and (3) ablate auxiliary KL punishment after the detection of revisitation. We respectively name them as NRT-ab-new-branch, NRT-ab-alpha, and NRT-ab-KL.

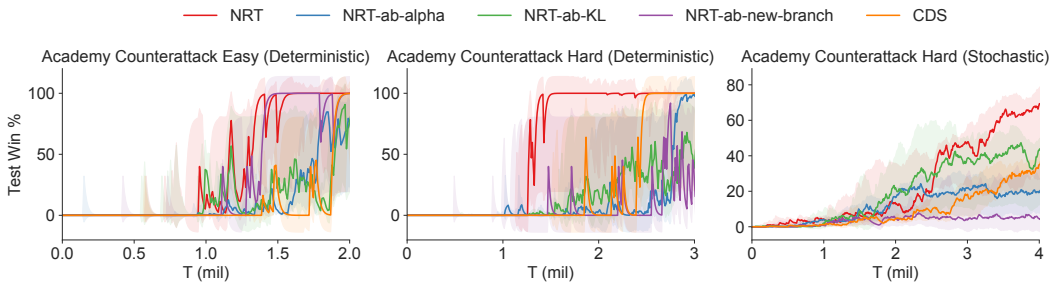

Figure 7: Ablation studies on three GRF tasks.

We compare NRT with its ablations on three representative tasks: `Academy_Counterattack_Easy` under the deterministic setting and `Academy_Counterattack_Hard` under both the deterministic and stochastic environment, as shown in Fig. 7. As for NRT-ab-new-branch, we notice an interesting phenomenon. In `Academy_Counterattack_Easy`, NRT-ab-new-branch performs similarly with NRT. However, in `Academy_Counterattack_Hard` under the deterministic setting, a more complex task, the performance of NRT-ab-new-branch is worse than NRT but still can win sometimes. In `Academy_Counterattack_Hard` under the stochastic setting, the most challenging task, the median winning rate of NRT-ab-new-branch during evaluation is almost zero. This phenomenon reveals the importance of constructing dynamically augmentation of neural network structure according to the degree of exploration in complex environments. The performance of NRT-ab-alpha and NRT-ab-KL in three tasks illustrate that the combined effect of our auxiliary supporting incentives makes our approach outperform vanilla CDS.

5.2 SMAC

In this section, we test our approach on SMAC, consisting of various maps with different agent numbers and various agent types. Previous work has achieved remarkable performance in many challenging tasks. However, their success heavily relays on dense rewards provided by the environment, which includes changes in the blood volume of our agents and opposing agents. In this paper, we consider SMAC tasks in the sparse reward setting. Agents will only receive rewards at the end of one episode. Agents will get +100 if they win, else get -1, which maintains the same as that in GRF.

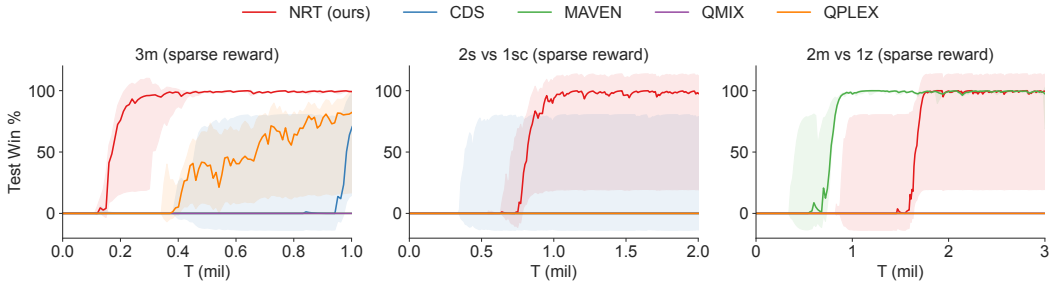

Figure 8: Comparison of our approach against baseline algorithms on SMAC in the sparse reward setting.

Fig. 8 demonstrates the comparison between our approach with baseline algorithms in three easy SMAC maps with sparse reward. QMIX achieves good performance with dense rewards (Rashid et al., 2018). However, vanilla QMIX can not learn any strategies to win in all three easy maps based on sparse rewards as shown in Fig. 8. Using QMIX as the mixing network, CDS can learn valuable strategies in `3m` with its intrinsic motivations as discussed in Sec. 2.2. However, CDS still learns nothing to win in `2m_vs_1z`. Our approach, adjusting intrinsic rewards of CDS based on the detection of revisitation, outperforms CDS in all three maps. The comparison between NRT and CDS supports our above discussion about one potential drawback of current intrinsic motivation methods, revisitation, which seriously influences exploration efficiency. QPLEX achieves good performance in

3m with its duplex dueling network architecture, but still learns nothing to win in other two maps. MAVEN achieves remarkable performance in 2m_vs_1z, but performs similar with QMIX in other two maps. Compared with QPLEX and MAVEN, NRT can adapt to all three maps, showing its exploration efficiency.

6 Related Work

Exploration Bonuses. Exploration is one key factor that determines the efficiency of deep reinforcement learning (Houthooft et al., 2016; Trott et al., 2019; Raileanu & Rocktäschel, 2020; Zintgraf et al., 2021; Chen et al., 2021). Starting from the classic ϵ-greedy action selector, numerous advanced algorithms are proposed to enhance the efficiency of exploration. Count-based exploration methods directly use visit counts to guide an agent's behavior towards reducing uncertainty (Strehl & Littman, 2008; Bellemare et al., 2016; Martin et al., 2017; Ostrovski et al., 2017; Tang et al., 2017; Machado et al., 2020). A representative method is Random Network Distillation (RND), using prediction errors to estimate count-based rewards (Burda et al., 2018b; Osband et al., 2018; 2019; Ciosek et al., 2019). The prediction errors are also used in Pathak et al. (2017); Burda et al. (2018a); Pathak et al. (2019); Dean et al. (2020) to achieve self-organized intrinsic motivations.

Exploration in the Multi-Agent Setting. Exploration is more crucial in the multi-agent setting, because the search space grows exponentially with the number of agents. Besides exploring the environment, we also need to consider diversity across agents to achieve sophisticated coordination. In the multi-agent setting, agents' exploration can be jointly encouraged (Mahajan et al., 2019; Gupta et al., 2021; Zheng et al., 2021; Liu et al., 2021), encouraged in pairs (Wang et al., 2020b; Ndousse et al., 2021), or independently encouraged for being special from the whole group (Jiang & Lu, 2021; Li et al., 2021). Exploration can also be encouraged through the factorization of roles (Wang et al., 2020a; 2021b). In this paper, we choose CDS (Li et al., 2021) as the intrinsic motivation for exploration because it is the current state-of-the-art algorithm in many challenging benchmarks.

Forgetting. Revisitation discussed in our paper also relates to the forgetting of previous policies, which is wildly discussed in lifelong learning with the multi-task setting (Rebuffi et al., 2017; Li & Hoiem, 2017; Rolnick et al., 2019; Von Oswald et al., 2019). Some advanced algorithms have studied this topic by extending the supervised regularization (Kirkpatrick et al., 2017) or replay (Isele & Cosgun, 2018; Yan et al., 2022) paradigms, exacerbating the stability-plasticity tension. Others, on the other hand, have proposed multi-stage processes in which the agent first applies existing knowledge to the current task and then incorporates newly acquired knowledge into a shared repository (Schwarz et al., 2018; Mendez et al., 2020). However, forgetting is rarely discussed in single-task and multi-agent reinforcement learning, which also has the possibility of forgetting during exploration. The key question is how to detect and forbid it automatically without any information about the stages agents are in during learning.

In this paper, we attempt to answer this question to enhance exploration efficiency. Ecoffet et al. (2019) and Ecoffet et al. (2021) intuitively show a hypothetical example of revisitation caused by detachment in intrinsic motivations. They solve it by storing all visited states and related policies to access. Before sampling, they will first check which state to return from the whole state space, which is challenging to execute in a large continuous search space, especially in multi-agent settings. In this paper, we empirically show policies' repeated revisitation in the multi-agent setting and solve it based on much fewer memories. Our approach maintains active detection and prevention of revisitation. We hope this paper can stimulate a rethinking of intrinsic motivations for more effective exploration in single-task multi-agent learning.

7 Closing Remarks

In this paper, we investigate the intrinsic motivation methods for multi-agent exploration, and find the revisitation issue that prevents these methods from achieving efficient exploration in complex tasks based on sparse rewards. For future work, we plan to study the interplay between the number of augmented branches and the scale of the proposed intrinsic rewards. We hope our work can encourage more studying on the limitation of current exploration methods based on intrinsic motivations to push forward the boundary of artificial intelligence.

REFERENCES

Adrià Puigdomènech Badia, Pablo Sprechmann, Alex Vitvitskyi, Daniel Guo, Bilal Piot, Steven Kapturowski, Olivier Tieleman, Martín Arjovsky, Alexander Pritzel, Andew Bolt, et al. Never give up: Learning directed exploration strategies. *arXiv preprint arXiv:2002.06038*, 2020.

Nolan Bard, Jakob N Foerster, Sarath Chandar, Neil Burch, Marc Lanctot, H Francis Song, Emilio Parisotto, Vincent Dumoulin, Subhodeep Moitra, Edward Hughes, et al. The hanabi challenge: A new frontier for ai research. *Artificial Intelligence*, 280:103216, 2020.

Marc Bellemare, Sriram Srinivasan, Georg Ostrovski, Tom Schaul, David Saxton, and Remi Munos. Unifying count-based exploration and intrinsic motivation. In *Advances in Neural Information Processing Systems*, pp. 1471–1479, 2016.

Yuri Burda, Harri Edwards, Deepak Pathak, Amos Storkey, Trevor Darrell, and Alexei A Efros. Large-scale study of curiosity-driven learning. *arXiv preprint arXiv:1808.04355*, 2018a.

Yuri Burda, Harrison Edwards, Amos Storkey, and Oleg Klimov. Exploration by random network distillation. *arXiv preprint arXiv:1810.12894*, 2018b.

Haipeng Chen, Wei Qiu, Han-Ching Ou, Bo An, and Milind Tambe. Contingency-aware influence maximization: A reinforcement learning approach. In *Uncertainty in Artificial Intelligence*, pp. 1535–1545. PMLR, 2021.

Kamil Ciosek, Vincent Fortuin, Ryota Tomioka, Katja Hofmann, and Richard Turner. Conservative uncertainty estimation by fitting prior networks. In *International Conference on Learning Representations*, 2019.

Christian Schroeder de Witt, Tarun Gupta, Denys Makoviichuk, Viktor Makoviychuk, Philip HS Torr, Mingfei Sun, and Shimon Whiteson. Is independent learning all you need in the starcraft multi-agent challenge? *arXiv preprint arXiv:2011.09533*, 2020.

Victoria Dean, Shubham Tulsiani, and Abhinav Gupta. See, hear, explore: Curiosity via audio-visual association. *Advances in Neural Information Processing Systems*, 33:14961–14972, 2020.

Adrien Ecoffet, Joost Huizinga, Joel Lehman, Kenneth O Stanley, and Jeff Clune. Go-explore: a new approach for hard-exploration problems. *arXiv preprint arXiv:1901.10995*, 2019.

Adrien Ecoffet, Joost Huizinga, Joel Lehman, Kenneth O Stanley, and Jeff Clune. First return, then explore. *Nature*, 590(7847):580–586, 2021.

Jakob Foerster, Francis Song, Edward Hughes, Neil Burch, Iain Dunning, Shimon Whiteson, Matthew Botvinick, and Michael Bowling. Bayesian action decoder for deep multi-agent reinforcement learning. In *International Conference on Machine Learning*, pp. 1942–1951, 2019.

Jakob N Foerster, Gregory Farquhar, Triantafyllos Afouras, Nantas Nardelli, and Shimon Whiteson. Counterfactual multi-agent policy gradients. In *Thirty-Second AAAI Conference on Artificial Intelligence*, 2018.

Tarun Gupta, Anuj Mahajan, Bei Peng, Wendelin Böhmer, and Shimon Whiteson. Uneven: Universal value exploration for multi-agent reinforcement learning. In *International Conference on Machine Learning*, pp. 3930–3941. PMLR, 2021.

Rein Houthooft, Xi Chen, Yan Duan, John Schulman, Filip De Turck, and Pieter Abbeel. Vime: Variational information maximizing exploration. In *Advances in Neural Information Processing Systems*, pp. 1109–1117, 2016.

David Isele and Akansel Cosgun. Selective experience replay for lifelong learning. In *Proceedings of the AAAI Conference on Artificial Intelligence*, volume 32, 2018.

Jiechuan Jiang and Zongqing Lu. The emergence of individuality. In *International Conference on Machine Learning*, pp. 4992–5001. PMLR, 2021.

James Kirkpatrick, Razvan Pascanu, Neil Rabinowitz, Joel Veness, Guillaume Desjardins, Andrei A Rusu, Kieran Milan, John Quan, Tiago Ramalho, Agnieszka Grabska-Barwinska, et al. Overcoming catastrophic forgetting in neural networks. *Proceedings of the national academy of sciences*, 114 (13):3521–3526, 2017.

Karol Kurach, Anton Raichuk, Piotr Stańczyk, Michał Zajac, Olivier Bachem, Lasse Espeholt, Carlos Riquelme, Damien Vincent, Marcin Michalski, Olivier Bousquet, et al. Google research football: A novel reinforcement learning environment. In *Proceedings of the AAAI Conference on Artificial Intelligence*, volume 34, pp. 4501–4510, 2020.

Vitaly Kurin, Maximilian Igl, Tim Rocktäschel, Wendelin Boehmer, and Shimon Whiteson. My body is a cage: the role of morphology in graph-based incompatible control. In *International Conference on Learning Representations*, 2020.

Chenghao Li, Tonghan Wang, Chengjie Wu, Qianchuan Zhao, Jun Yang, and Chongjie Zhang. Celebrating diversity in shared multi-agent reinforcement learning. *arXiv e-prints*, pp. arXiv–2106, 2021.

Zhizhong Li and Derek Hoiem. Learning without forgetting. *IEEE transactions on pattern analysis and machine intelligence*, 40(12):2935–2947, 2017.

Iou-Jen Liu, Unnat Jain, Raymond A Yeh, and Alexander Schwing. Cooperative exploration for multi-agent deep reinforcement learning. In *International Conference on Machine Learning*, pp. 6826–6836. PMLR, 2021.

Ryan Lowe, Yi Wu, Aviv Tamar, Jean Harb, OpenAI Pieter Abbeel, and Igor Mordatch. Multi-agent actor-critic for mixed cooperative-competitive environments. In *Advances in Neural Information Processing Systems*, pp. 6379–6390, 2017.

Xiaoteng Ma, Yiqin Yang, Chenghao Li, Yiwen Lu, Qianchuan Zhao, and Jun Yang. Modeling the interaction between agents in cooperative multi-agent reinforcement learning. In *Proceedings of the 20th International Conference on Autonomous Agents and MultiAgent Systems*, pp. 853–861, 2021.

Marlos C Machado, Marc G Bellemare, and Michael Bowling. Count-based exploration with the successor representation. In *Proceedings of the AAAI Conference on Artificial Intelligence*, volume 34, pp. 5125–5133, 2020.

Anuj Mahajan, Tabish Rashid, Mikayel Samvelyan, and Shimon Whiteson. Maven: Multi-agent variational exploration. In *Advances in Neural Information Processing Systems*, pp. 7611–7622, 2019.

Jarryd Martin, Suraj Narayanan Sasikumar, Tom Everitt, and Marcus Hutter. Count-based exploration in feature space for reinforcement learning. *arXiv preprint arXiv:1706.08090*, 2017.

Jorge Mendez, Boyu Wang, and Eric Eaton. Lifelong policy gradient learning of factored policies for faster training without forgetting. *Advances in Neural Information Processing Systems*, 33: 14398–14409, 2020.

Kamal K Ndousse, Douglas Eck, Sergey Levine, and Natasha Jaques. Emergent social learning via multi-agent reinforcement learning. In *International Conference on Machine Learning*, pp. 7991–8004. PMLR, 2021.

Frans A Oliehoek, Christopher Amato, et al. *A concise introduction to decentralized POMDPs*, volume 1. Springer, 2016.

Ian Osband, John Aslanides, and Albin Cassirer. Randomized prior functions for deep reinforcement learning. *Advances in Neural Information Processing Systems*, 31, 2018.

Ian Osband, Benjamin Van Roy, Daniel J Russo, Zheng Wen, et al. Deep exploration via randomized value functions. *J. Mach. Learn. Res.*, 20(124):1–62, 2019.

Georg Ostrovski, Marc G Bellemare, Aäron van den Oord, and Rémi Munos. Count-based exploration with neural density models. In *Proceedings of the 34th International Conference on Machine Learning-Volume 70*, pp. 2721–2730. JMLR. org, 2017.

Deepak Pathak, Pulkit Agrawal, Alexei A Efros, and Trevor Darrell. Curiosity-driven exploration by self-supervised prediction. In *International Conference on Machine Learning*, pp. 2778–2787, 2017.

Deepak Pathak, Dhiraj Gandhi, and Abhinav Gupta. Self-supervised exploration via disagreement. In *International conference on machine learning*, pp. 5062–5071. PMLR, 2019.

Roberta Raileanu and Tim Rocktäschel. Ride: Rewarding impact-driven exploration for procedurally-generated environments. *arXiv preprint arXiv:2002.12292*, 2020.

Tabish Rashid, Mikayel Samvelyan, Christian Schroeder Witt, Gregory Farquhar, Jakob Foerster, and Shimon Whiteson. Qmix: Monotonic value function factorisation for deep multi-agent reinforcement learning. In *International Conference on Machine Learning*, pp. 4292–4301, 2018.

Sylvestre-Alvise Rebuffi, Alexander Kolesnikov, Georg Sperl, and Christoph H Lampert. icarl: Incremental classifier and representation learning. In *Proceedings of the IEEE conference on Computer Vision and Pattern Recognition*, pp. 2001–2010, 2017.

David Rolnick, Arun Ahuja, Jonathan Schwarz, Timothy Lillicrap, and Gregory Wayne. Experience replay for continual learning. *Advances in Neural Information Processing Systems*, 32, 2019.

Mikayel Samvelyan, Tabish Rashid, Christian Schroeder de Witt, Gregory Farquhar, Nantas Nardelli, Tim GJ Rudner, Chia-Man Hung, Philip HS Torr, Jakob Foerster, and Shimon Whiteson. The starcraft multi-agent challenge. *arXiv preprint arXiv:1902.04043*, 2019.

Jonathan Schwarz, Wojciech Czarnecki, Jelena Luketina, Agnieszka Grabska-Barwinska, Yee Whye Teh, Razvan Pascanu, and Raia Hadsell. Progress & compress: A scalable framework for continual learning. In *International Conference on Machine Learning*, pp. 4528–4537. PMLR, 2018.

Kyunghwan Son, Daewoo Kim, Wan Ju Kang, David Earl Hostallero, and Yung Yi. Qtran: Learning to factorize with transformation for cooperative multi-agent reinforcement learning. In *International Conference on Machine Learning*, pp. 5887–5896, 2019.

Kyunghwan Son, Sungsoo Ahn, Roben Delos Reyes, Jinwoo Shin, and Yung Yi. Qtran++: Improved value transformation for cooperative multi-agent reinforcement learning, 2020.

Alexander L Strehl and Michael L Littman. An analysis of model-based interval estimation for markov decision processes. *Journal of Computer and System Sciences*, 74(8):1309–1331, 2008.

Peter Sunehag, Guy Lever, Audrunas Gruslys, Wojciech Marian Czarnecki, Vinicius Zambaldi, Max Jaderberg, Marc Lanctot, Nicolas Sonnerat, Joel Z Leibo, Karl Tuyls, et al. Value-decomposition networks for cooperative multi-agent learning based on team reward. In *Proceedings of the 17th International Conference on Autonomous Agents and MultiAgent Systems*, pp. 2085–2087. International Foundation for Autonomous Agents and Multiagent Systems, 2018.

Haoran Tang, Rein Houthooft, Davis Foote, Adam Stooke, OpenAI Xi Chen, Yan Duan, John Schulman, Filip DeTurck, and Pieter Abbeel. # exploration: A study of count-based exploration for deep reinforcement learning. In *Advances in neural information processing systems*, pp. 2753–2762, 2017.

Alexander Trott, Stephan Zheng, Caiming Xiong, and Richard Socher. Keeping your distance: Solving sparse reward tasks using self-balancing shaped rewards. *Advances in Neural Information Processing Systems*, 32, 2019.

Johannes Von Oswald, Christian Henning, João Sacramento, and Benjamin F Grewe. Continual learning with hypernetworks. *arXiv preprint arXiv:1906.00695*, 2019.

Jianhao Wang, Zhizhou Ren, Terry Liu, Yang Yu, and Chongjie Zhang. Qplex: Duplex dueling multi-agent q-learning. *International Conference on Learning Representations (ICLR)*, 2021a.

Tonghan Wang, Heng Dong, Victor Lesser, and Chongjie Zhang. Roma: Multi-agent reinforcement learning with emergent roles. In *Proceedings of the 37th International Conference on Machine Learning*, 2020a.

Tonghan Wang, Jianhao Wang, Wu Yi, and Chongjie Zhang. Influence-based multi-agent exploration. In *Proceedings of the International Conference on Learning Representations (ICLR)*, 2020b.

Tonghan Wang, Tarun Gupta, Anuj Mahajan, Bei Peng, Shimon Whiteson, and Chongjie Zhang. Rode: Learning roles to decompose multi-agent tasks. In *Proceedings of the International Conference on Learning Representations (ICLR)*, 2021b.

Qingsen Yan, Dong Gong, Yuhang Liu, Anton van den Hengel, and Javen Qinfeng Shi. Learning bayesian sparse networks with full experience replay for continual learning. In *Proceedings of the IEEE/CVF Conference on Computer Vision and Pattern Recognition*, pp. 109–118, 2022.

Chao Yu, Akash Velu, Eugene Vinitsky, Yu Wang, Alexandre Bayen, and Yi Wu. The surprising effectiveness of ppo in cooperative, multi-agent games. *arXiv preprint arXiv:2103.01955*, 2021.

Chongjie Zhang and Victor Lesser. Coordinating multi-agent reinforcement learning with limited communication. In *Proceedings of the 2013 international conference on Autonomous agents and multi-agent systems*, pp. 1101–1108. International Foundation for Autonomous Agents and Multiagent Systems, 2013.

Zhi Zhang, Jiachen Yang, and Hongyuan Zha. Integrating independent and centralized multi-agent reinforcement learning for traffic signal network optimization. *arXiv preprint arXiv:1909.10651*, 2019.

Lulu Zheng, Jiarui Chen, Jianhao Wang, Jiamin He, Yujing Hu, Yingfeng Chen, Changjie Fan, Yang Gao, and Chongjie Zhang. Episodic multi-agent reinforcement learning with curiosity-driven exploration. *Advances in Neural Information Processing Systems*, 34:3757–3769, 2021.

Luisa M Zintgraf, Leo Feng, Cong Lu, Maximilian Igl, Kristian Hartikainen, Katja Hofmann, and Shimon Whiteson. Exploration in approximate hyper-state space for meta reinforcement learning. In *International Conference on Machine Learning*, pp. 12991–13001. PMLR, 2021.

A EXPERIMENT SETTING

The visualization of the initial position of each agent is shown in Fig. 9. The difficulty of scenarios increases from `Academy_3_vs_1_with_Keeper` to `Academy_Counterattack_Hard` based on a noticeable difference between the number of agents and the initial distance of each agent to the goal and opposing players.

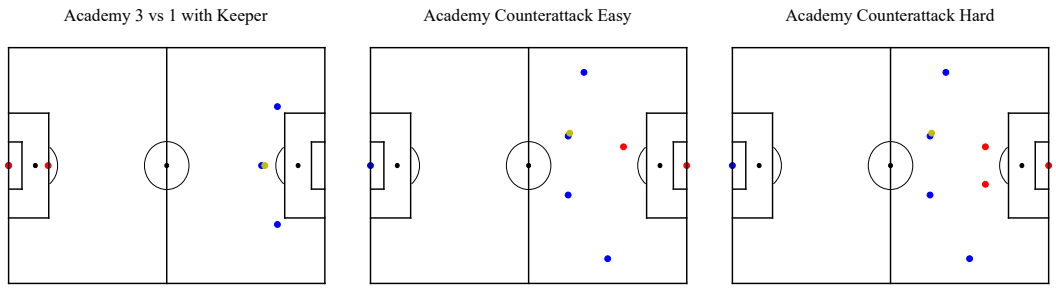

Figure 9: Visualization of the initial position of each agent in three GRF scenarios considered in our paper, where blue points represent our controlled team, red points represent the opposing team, and yellow point represents the ball.

B ARCHITECTURE AND HYPER-PARAMETERS

In this paper, we use simple network structures for the local Q-networks and the mixing networks as baselines. Agents use a partially shared module to represent local Q-functions as CDS (Li et al., 2021). Following the setting of CDS, agents share a trajectory encoding network made up of two layers: a fully connected layer followed by a GRU layer with a 64-dimensional hidden state for individual Q-functions. Following the trajectory encoding network, all agents share a one-layer Q network, with each agent having its own Q network with the same structure as the shared Q network. To estimate the global action values, we use QMIX-style mixing networks, which include two 32-dimensional hidden layers activated by ReLU. Hypernetworks condition on global states to generate mixing network parameters. These options apply to QMIX Rashid et al. (2018) as well.

All experiments are optimized using RMSprop with a learning rate of 5×10^{-4}, γ of 0.99, and no momentum or weight decay. We use ϵ-greedy with ϵ anneals linearly from 1.0 to 0.05 over 50K time steps and keep constant for the rest of the training while selecting actions. We will evaluate the latest policies 32 times every 10k steps to calculate the average winning rate. For our approach, all baselines and ablations, we introduce a prioritized replay buffer with the same α of 0.3 and use TD(0.8) while calculating target values.

The intrinsic motivation introduced in CDS includes three hyper-parameters: β, β_1, and β_2, with another hyper-parameter λ controls the weight of L1 regularization on independent local Q-networks. In this paper, we roughly fine-tune these hyper-parameters while ensuring CDS uses the same hyper-parameters during comparison. For the maze game, we use $\{\beta, \beta_1, \beta_2\ \lambda\}$ as $\{0.15, 0.5, 0.5, 0.01\}$. For all GRF scenarios, we use $\{\beta, \beta_1, \beta_2, \lambda\}$ as $\{0.05, 0.5, 1.0, 0.1\}$, which is the same as the original CDS setting in GRF environments.

In our approach, we introduce several special hyper-parameters and some basic settings to establish our framework. δ in Definition 1 is fixed as 4 in all experiments. η in Eq. 3 is fixed to 1 in all experiments. To reduce the size of the replay buffer loading trajectories to calculate α, we will save trajectories every ten times. The weight of L1 normalization on independent mixing networks is fixed to 0.1 in all experiments. $\{L_1, L_2, \beta_p\}$ is set to $\{0.5, 2.0, 10^{-3}\}$ for the maze game. For all GRF scenarios, β_p is set to 0.001. $\{L_1, L_2\}$ is set to $\{0.5, 2.0\}$ for the scenario `Academy_Counterattack_Easy` based on both stochastic and deterministic environment setting. Meanwhile, $\{L_1, L_2\}$ is set to $\{1.0, 2.0\}$ for other scenarios. For all SMAC maps, $\{L_1, L_2, \beta_p\}$ is set to $\{1.0, 4.0, 10^{-3}\}$.

We use the codes provided by the authors for all baseline algorithms.

B.1 SUPPLEMENTARY INTERPRETATION OF NRT'S DYNAMICALLY AUGMENTED NEURAL NETWORK STRUCTURE

In this paper, at the beginning of learning, when no revisitation is detected, we maintain local Q-networks as CDS (Li et al., 2021) with a QMIX-style mixing network to estimate Q_{tot}.

Based on each revisitation, we separate the whole joint observation space into sub-spaces with Eq. 3. In this section, for convenience, we use sub-space to represent sub- joint observation space which is dynamically separated along with the detection of revisitaion. To provide sufficient policy representation capacity, we dynamically augment the neural network structure for each sub-space as shown in Fig. 2.

The last layers of agents' local Q-networks are independent across sub-spaces, while the previous layers are shared for benefits in learning efficiency from parameter sharing. Here we name the augmented last layer of agents' local Q-networks as the *augmented local-Q branch* activated in the sub-space of related revisitation. The original last layer of agents' local Q-networks initialized at the beginning of learning is named as *default local-Q branch* activated when no revisitation is detected or in the sub-space related to no revisitation.

For achieving sufficient representational capacity of the mixing network, we augment it along with augmentations of local Q-networks as shown in Fig. 2.

The original QMIX (Rashid et al., 2018) calculates Q_{tot} with:

$$Q_{tot} = ([Q_1, ..., Q_n]W_1 + b_1)W_2^T + b_2, \tag{6}$$

where Q_i is the local Q-value of agent $i \in I$, W_1 is a $n \times m$ matrix, b_1 and W_2 are vectors with m dimensions, b_2 is a variable with 1 dimension. W_1 and W_2 are both with non-negative values. W_1, W_2, b_1, and b_2 are all outputs of several hypernetworks with the state as input.

However, the shared mixing network might not have enough capacity while the number of local-Q branches increasing. Thus we further expand the mixing network. Our QMIX-style mixing network is

$$\begin{aligned} Q_{tot} &= ([Q_1, ..., Q_n]W_1 + b_1)(W_2^T + W_B^T) + b_2 + b_B \\ &= (([Q_1, ..., Q_n]W_1 + b_1)W_2^T + b_2) + (([Q_1, ..., Q_n]W_1 + b_1)W_B^T + b_B) \\ &= Q_{tot}^S + Q_{tot}^I, \end{aligned} \tag{7}$$

where W_B is a vector with m dimensions and b_B is a variable with 1 dimension. Q_{tot}^S is shared among sub-spaces with shared parameters W_1, b_1, W_2, and b_2. Q_{tot}^I is an individual part of each sub-space's mixing network with individual parameters W_B and b_B. Here we name the augmented W_B and b_B related to each revisitation as the *augmented mixing network branch*. The original W_B and b_B initialized at the beginning of learning is named as *default mixing network branch* activated when no revisitation is detected or the sub-space related to no revisitation.

In its current form, the mixing network relays on Q_{tot}^S or Q_{tot}^I arbitrarily. On the contrary, we expect credit assignments across agents (achieved by the mixing network) to not differ too much between sub-spaces for stability. Thus we add an L1 regularization to mixing network branches to encourage them to work only when necessary.

The original QMIX (Rashid et al., 2018) train Q_{tot} with

$$\mathcal{L}(\theta) = \sum_{i=1}^{b} \left[\left(y_i^{tot} - Q_{tot}(\boldsymbol{\tau}, \mathbf{u}, s; \theta) \right)^2 \right], \tag{8}$$

where $y^{tot} = r + \gamma \max_{\mathbf{u}'} Q_{tot}(\boldsymbol{\tau}', \mathbf{u}', s'; \theta^-)$, θ^- are the parameters of a target network as in DQN, and b is the batch size of transitions sampled from the replaybuffer.

In this paper, we train Q_{tot} with

$$\mathcal{L}(\theta) = \sum_{i=1}^{b} \left[\left(y_i^{tot} - Q_{tot}(\boldsymbol{\tau}, \mathbf{u}, s; \theta) \right)^2 \right] + \sum_{i=1}^{b} ||Q_{tot}^{I,-}||_1, \tag{9}$$

where (1) $y^{tot} = r^E + r^I + \gamma \max_{\mathbf{u}'} Q_{tot}(\boldsymbol{\tau}', \mathbf{u}', s'; \theta^-)$, r^E is environmental rewards, and r^I can be any intrinsic rewards. In this paper, we use intrinsic rewards from CDS (Li et al., 2021), which is named as r^I_{CDS}. (2) $Q_{tot}^{I,-} = (\texttt{stopgrad}([Q_1, ..., Q_n]W_1 + b_1))W_B^T + b_B$ is an additional regularization loss item. `stopgrad` is used to stop gradient back-propagation. Thus we can only regularize parameters related to each mixing network branch.

During decentralized execution, one agent can only obtain its local observation. Thus, we introduce the marginal condition Eq. 4 based on Eq. 3 to guide each agent to select local-Q branches for sampling as shown in Algorithm 1. To maintain consistency between sampling and training, Algorithm 1 is also used to select each agent's local Q-network branches while training. To solve the question about how to switch augmented mixing network branches when agents switch various local-Q branches at one time step, each augmented mixing network branch will be activated only when more than half of agents choose the corresponding augmented local-Q branch. Otherwise, the default mixing network branch is switched.

Algorithm 1 The sampling process of NRT

```
while Simulating do
    if no augmented local-Q branches then
        All agents activate the default local-Q branch to select actions
    else
        for agent i ∈ I do
            for augmented branch id b from the earliest created branch to the latest created branch do
                if o_i ∈ Ω_b^i based on Eq. 4 then
                    Agent i activates the b th augmented local-Q branch to select actions and stops
                    searching augmented branches.
                end if
            end for
            if no augmented local-Q branch is activated by agent i then
                Agent i activates the default local-Q branch to select actions.
            end if
        end for
    end if
end while
Return trajectories for training.
```

C Experimental Details

C.1 JS Distances Calculated During Training in GRF

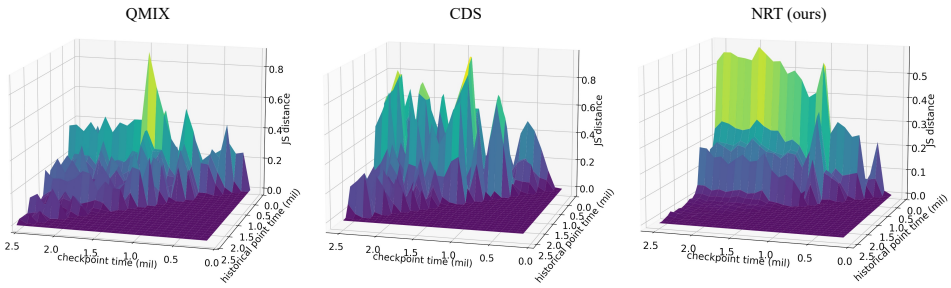

Figure 10: JS distances calculated during training in `Academy_Counterattack_Hard` under the deterministic setting

We further show JS distances calculated during training in `Academy_Counterattack_Hard` under the deterministic setting as a representative of GRF environments. The definition of the x-y axis is the same as that introduced in Sec. 4. Similar to our toy maze environment, JS distances between historical points and checkpoints periodically fluctuate under the training of QMIX and CDS, as shown in Fig. 10 left and middle. Meanwhile, under our approach's guidance of preventing revisitation, policies learned in complex environments achieve stable improvement, as shown in Fig. 10 right. Taking advantage from stable improved exploration, our approach achieves outstanding performance in challenging GRF scenarios.

C.2 The 2D-Color Plot of JS Distances During Training

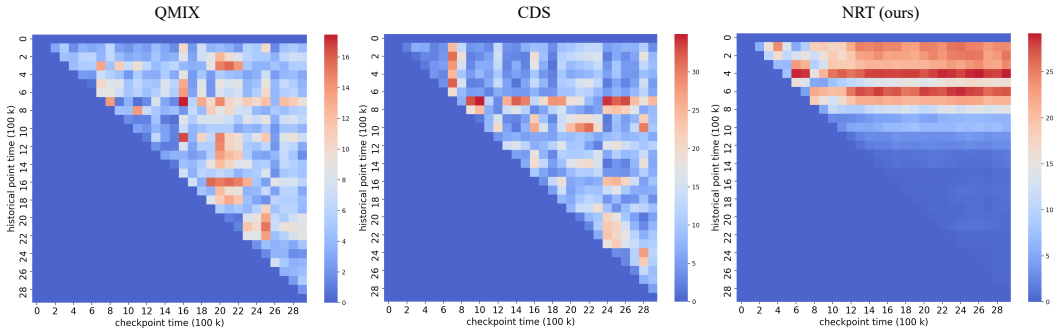

Figure 11: The 2D-color plot of Fig. 1.

We demonstrate the 2D-Color Plot of Fig. 1 as shown in Fig. 11 for readers to follow our work's motivations easier. During learning, we will store the joint observation distribution induced by the joint policy π every 100k time steps, named historical point time (the y-axis in Fig. 11). Meanwhile, for every 100k time step, we will calculate the JS distance between the current distribution and all historical points, named checkpoint time (the x-axis in Fig. 11). Half of each picture in Fig. 11 is printed in the same color. That is because checkpoint time is always larger than historical times while calculating the JS distances. For each historical point, it is compared with checkpoints after it every 100k time steps. In Fig. 11 right, most JS distances are large and stable until coverage to the optimal strategy, after our approach detects and solves revisitation at the early period of learning.

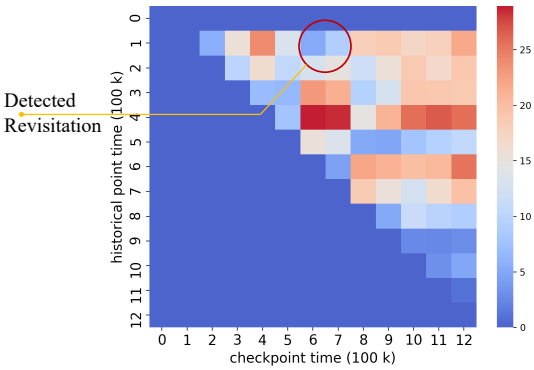

Figure 12: The 2D-color plot of JS distances between polices learned by our approach until converge.

In Fig. 12, we show and enlarge a part of Fig. 11 right to demonstrate our approach's learning progress before coverage clearly. *Through the whole learning period, revisitation means that the exploration achieved at one learning period is actually driving the joint policy to be similar to some historical policies.* For example, in Fig. 12, if we choose the joint observation distribution counted at 300k time-step as the historical point, checkpoints at 400k and 500k time-step indicate that intrinsic motivations are driving agents to explore the environment. However, if we choose the joint observation distribution counted at 100k time-step as the historical point, checkpoints at 400k and 500k time-step indicate that intrinsic motivations are driving agents to re-explore the sub-space that has been explored at 100k time-step. In this paper, we call this phenomenon revisitation and attempt to solve it with (1) augmented neural networks for sufficient policy representation capacity, (2) adjusted intrinsic motivation weight according to joint observation novelty compared with each revisitation historical point, and (3) further punishment of revisitation based on KL divergence. Based on these novelties, our approach forbids revisitation to occur again and achieves the optimal strategy in the maze exploration task by driving agents to explore away from both 100k time-step and 300k time-step, indicating reliable exploration efficiency.

As for baselines such as QMIX (explores with ϵ-greedy) and CDS (explores with intrinsic motivations), revisitation occurs periodically, which heavily influences exploration efficiency and causes agents to be stacked nearing the fixed initial points as shown in Fig. 4.

C.3 Will the Size of Replay Buffer Influence Revisitaion?

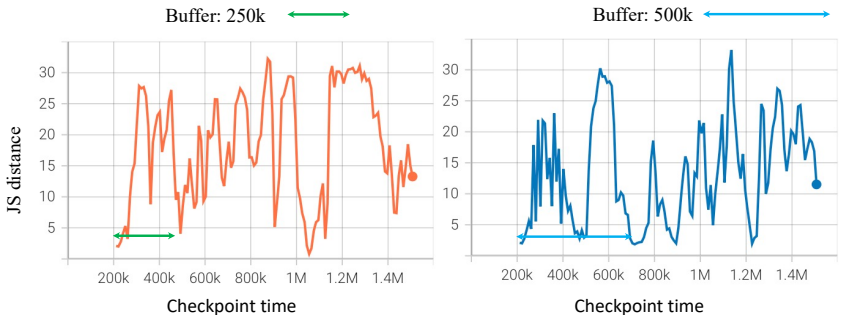

Figure 13: JS distances calculated during training with the CDS algorithm in our maze environment based on historical point at 200k time steps

Coming up with the phenomenon of revisitation based on intrinsic motivations is one natural question: Which role does the replay buffer play in revisitation? Here we still use CDS as an example of intrinsic motivations and test it in our maze environment. *Fig. 13 demonstrates that the size of replay buffer has trivial influence on revisitaion.* In Fig. 13 left, it seems that revisitation occurs according to the size of the replay buffer. However, after we multiply the replay buffer's size from 250k time steps to 500k time steps, the interval of periodical revisitation is similar to that with smaller replay buffer as shown in Fig. 13 right. Thus, in this paper, we choose to fix our replay buffer's size as baselines and adjust intrinsic motivations with augmented policy representation capacity.

C.4 Experimental Results Plotted with Means and Standard Deviations

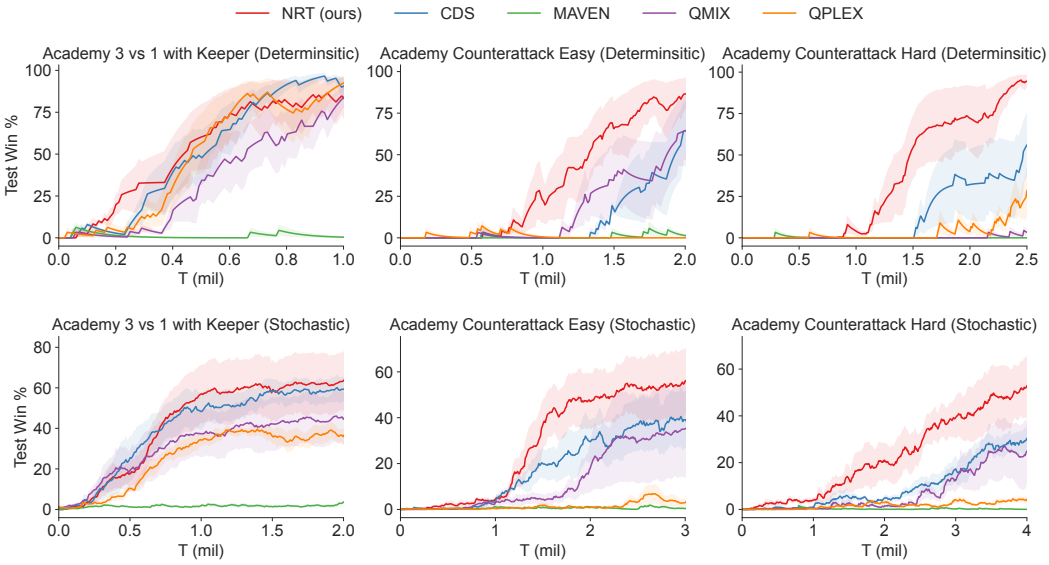

Figure 14: Comparison of our approach against baseline algorithms on GRF with deterministic environment seeds or stochastic environment seeds.

We re-plot our experimental results with means and standard deviations as shown in Fig. 14 and Fig. 15. The comparison between our algorithm and baseline is consistent with that measured with

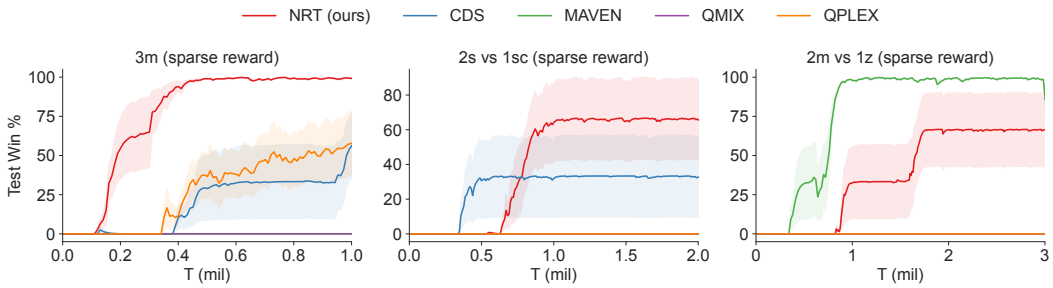

Figure 15: Comparison of our approach against baseline algorithms on SMAC with sparse rewards.

median performance. In general, our approach achieves better performance in 4 out of 6 GRF scenarios (slightly better in `Academy_3_vs_1_with_Keeper` based on the stochastic environment) and 2 out of 3 SMAC maps.